Supplementary Material (ESI) for *Physical Chemistry Chemical Physics*

Electrodeposited noble metal particles in polyelectrolyte multilayer matrix as electrocatalyst for oxygen reduction studied using SECM

Yan Shen, Markus Träuble, Gunther Wittstock*

Carl von Ossietzky University Oldenburg, Faculty of Mathematics and Natural Sciences, Center of Interface Science (CIS), Department of Pure and Applied Chemistry and Institute of Chemistry and Biolgy of the Marine Environment (ICBM), D-26111 Oldenburg, Germany

Supporting information 1: CV of Au electrode in 0.1 M H_2SO_4

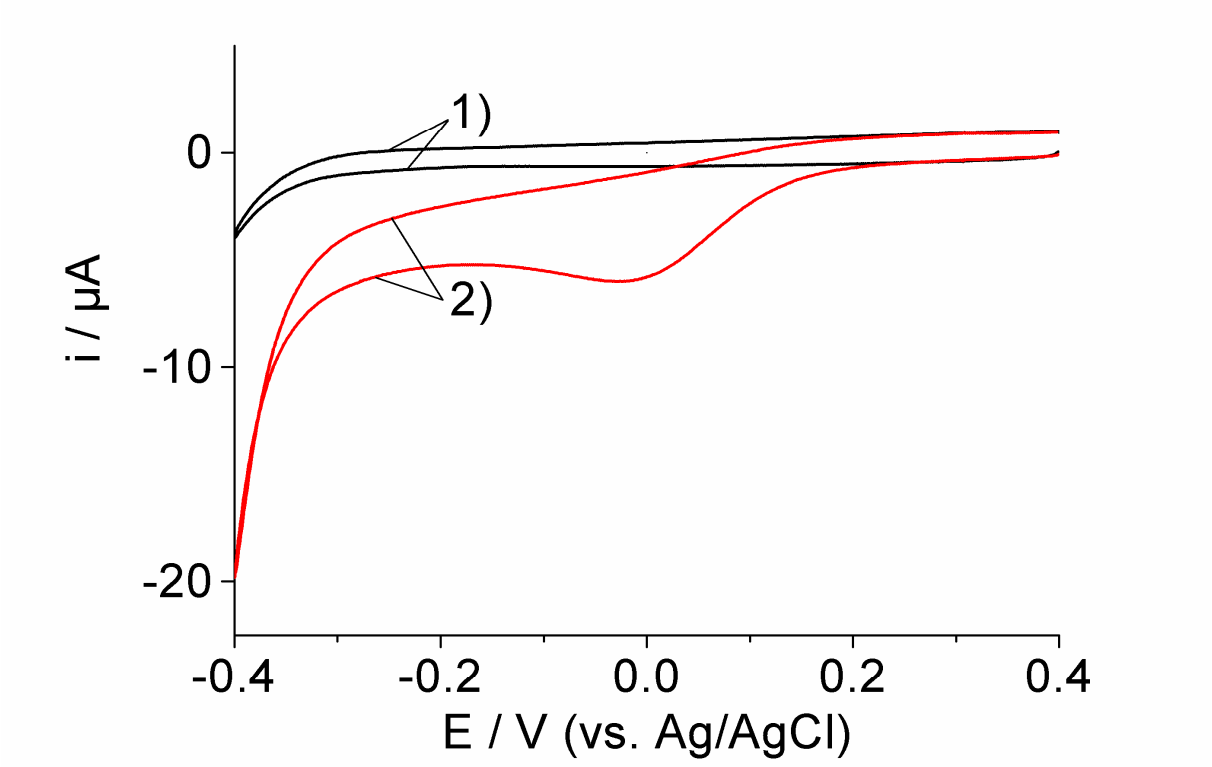

Figure S1-1: CV of gold electrode in 1) deaerated and 2) air-saturated 0.1 M H_2SO_4 solution, scan rate: 0.1 V/s.

Supporting information 2: CV of massive Pt and Pt cluster-modified electrodes in 0.1 M H_2SO_4

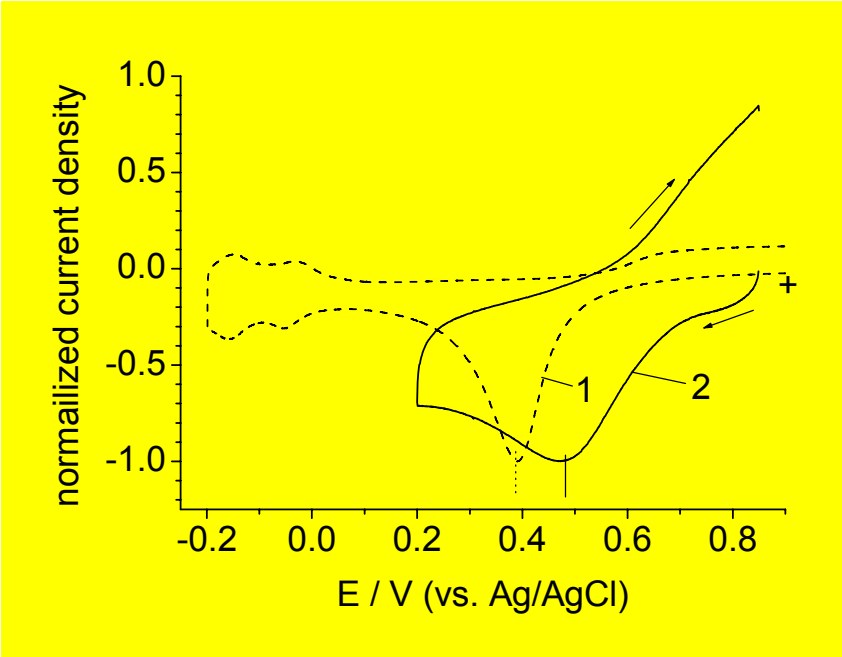

Fig. S2-1: CVs of oxygen reduction at bulk Pt electrode (curve 1) and Pt cluster modified Au electrode (curve 2) in 0.1 M H_2SO_4 saturated with air. Scan rate: 0.1 V s^{-1}.

The oxygen reduction peak occurs at about 100 mV more positive potentials than at the Pt bulk electrodes.

Supporting information 3: Effect of the uncertainty of the working distance on the obtained fitting results

The way of positioning the microelectrode vertically was used in order to avoid the need for changing the UME potential which resulted ain a more stable response. It introduced, however, a positional uncertainty in *d*. From many experiments also with other system we estimate that this uncertainty can amount to ± 3 µm. This is large when working in the SECM feedback mode, but it is rather less important when working in the generation-collection mode at $d \geq 50$ µm as done here when extracting effective rate constants. To illustrate this finding, we fitted the data in Figures 5 and 7 of the manuscript using *d* values incremented and decremented by 3 µm. (Figure S3-1)

Modified Distance *d'*	**Figure 5 of manuscript**	**Figure 7 of manuscript**
d' = *d* - 3 µm	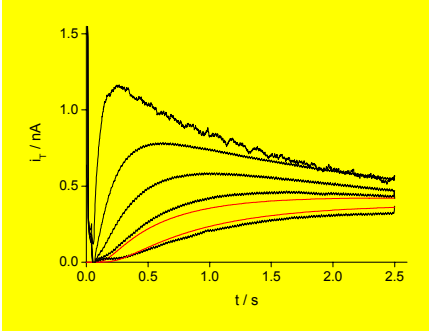	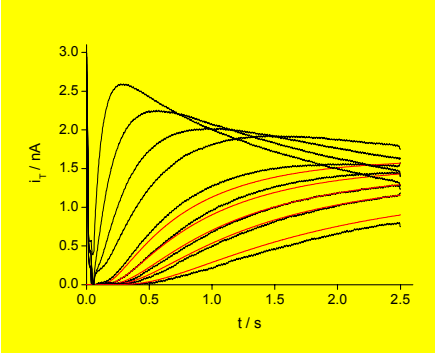
d' = *d* + 3 µm	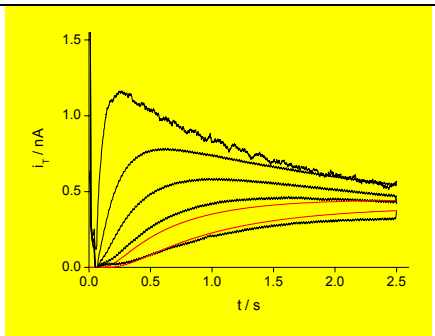	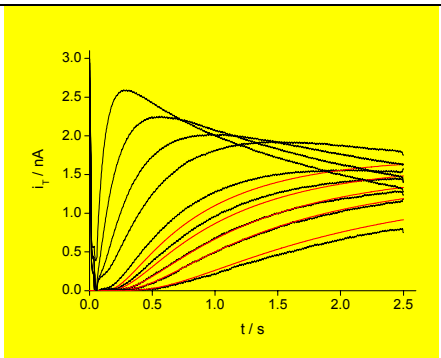

Figure S3-1: Fits of the experimental data of Figure 5 and Figure 7 with distances incremented and decremented by 3 µm.

The calculated curves describe the experimental values as well as the curves in the manuscript. The obtained effective rate constants are compiled in Tables S3-1 and S3-2.

Table S3-1: Effective rate constants obtained from a fit of the curve bundle in Figure 5 of the manuscript with a common set of effective rate constants under variation of the working distance.

Modified distance *d'*	k_1 / (cm s^{-1})	k_2 / (cm s^{-1})	k_3 / (cm s^{-1})
d' = *d*-3µm	0.00141	0.01192	0.00305
d' = *d* (Manuscript)	0.00140	0.0120	0.00306
d' = *d*+3µm	0.00167	0.0126	0.00316

Table S3-2: Effective rate constants obtained from a fit of the curve bundle in Figure 7 of the manuscript with a common set of effective rate constants under variation of the working distance.

Modified distance d'	k_1 / (cm s^{-1})	k_2 / (cm s^{-1})	k_3 / (cm s^{-1})
$d' = d$-3µm	0.00562	0.00863	0.00246
$d' = d$ (Manuscript)	0.00534	0.00719	0.00307
$d' = d$+3µm	0.00641	0.00823	0.00255

The influence of the distance uncertainty can be seen when summarizing the effective rate constants to the paramter $x(H_2O_2)$ as done in the main manuscript. Figure 10 of the manuscript is reproduced here with additional curves that would result from errors in estimating the working distance of ± 3 µm (Figure S3-2).

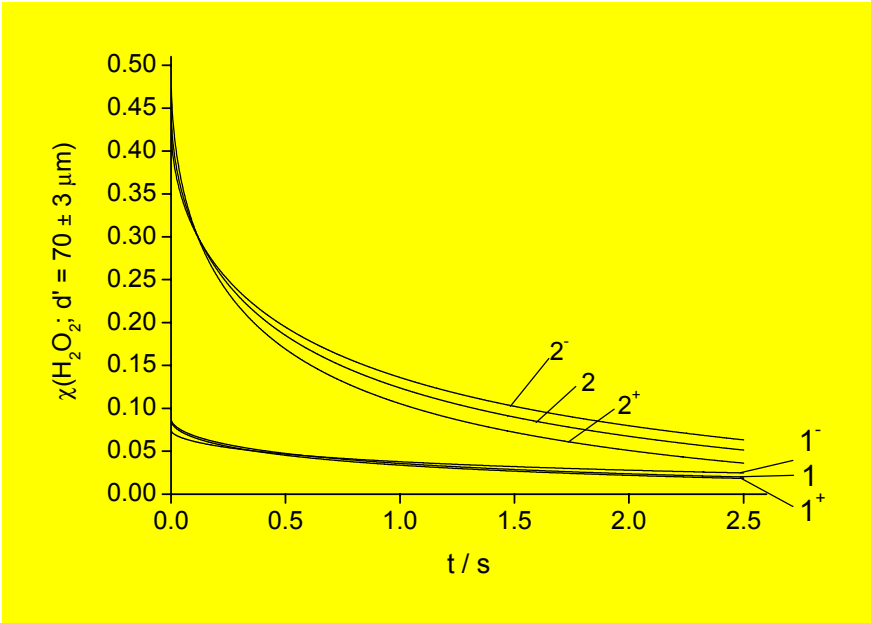

Figure S3-2: Calculated $\chi(H_2O_2)$ values for the ORR at at Au/(PDDA/PSS)4.5/Pd_{500s} (1) and Au/(PDDA/PSS)4.5/Pd_{800s} (2). Curve 1 was obtained from the experimental transients in Figure 5; Curve 2 was obtained from Figure 7 for d = 70 µm.. The curves with labels 1^+ and 2^+ were calculated assuming $d' = d + 3$ µm = 73 µm , the curves 1^- and 2^- were calculated with $d' = d$ - 3 µm = 67 µm.